J. Fluid Mech. (1975), *vol.* 69, *part* 3, *pp.* 539–563
Printed in Great Britain

Electro-convection in a dielectric liquid layer subjected to unipolar injection

By J. C. LACROIX, P. ATTEN
Laboratoire d'Electrostatique, CNRS, Grenoble, France

AND E. J. HOPFINGER
Laboratoire de Mécanique des Fluides (Laboratoire associé au CNRS),
Université de Grenoble, France

(Received 12 July 1974)

The problem of electric charge convection in a dielectric liquid layer of high ionic purity, when subjected to unipolar injection, is in many ways analogous to that of thermal convection in a horizontal fluid layer heated from below, although no formal analogy can be established. The problem treated is intrinsically more nonlinear than the thermal problem. We consider two asymptotic states of convection: one where the whole motion is dominated by viscosity, and one where inertial effects dominate. In each state, two or three spatial regions are distinguished. From the approximate equations that hold in the different regions, information about the variation of the different quantities with distance from the injector is obtained, and further approximations permit us to establish the dependence of the current density ratio I/I_0 (called the *electric Nusselt number*) on the stability parameter $T = M^2R = \epsilon\phi_0/K\rho\nu$, and on $1/R = \nu/K\phi_0$, which is an equivalent Prandtl number (ϵ is the permittivity, ρ the fluid density, K the mobility, ν the kinematic viscosity, and ϕ_0 the applied voltage). In the viscous state, the analysis gives $I/I_0 \propto T^{\frac{1}{2}}$; in the inertial state the law $I/I_0 \propto (T/R)^{\frac{1}{4}} = M^{\frac{1}{2}}$ is obtained. Since M is independent of the applied voltage, the latter law shows the saturation in the electric Nusselt number observed in earlier experiments. The transition in the states is associated with a transition number $(MR)_T \simeq 30$, which is an electric Reynolds number, related to an ordinary Reynolds number of about 10.

The experimental results, obtained in liquids of very different viscosities and dielectric constants, verify these theoretical predictions; further, they yield more precise numerical coefficients. As for the transition criteria, the experiments confirm that the viscous and inertial effects are of the same order when $Re \simeq 10$. It was also possible to determine roughly the limits of the viscous and inertial states. The viscous analysis remains valid up to a Reynolds number of about 1; the inertial state can be considered valid down to a Reynolds number of 60. Schlieren observations show that the motion has the structure of very stable hexagonal cells at applied voltages just above the critical voltage, which are transformed into unstable filaments when the voltage is increased further. At even higher voltages, the motion finally breaks down into turbulence. It may be

of interest to point out that, when $M < 3$, the electric Nusselt number approaches 1, which is equivalent to the situation in thermal convection at low Prandtl numbers.

1. Introduction

In dielectric liquids with a high degree of ionic purity, electrical conduction results from charge carriers, created by processes on the electrodes, rather than dissociation processes in the bulk of the liquid. The current associated with this production of charge on the electrodes is referred to as *injection current*. The resulting space charge gives rise to a Coulomb force which, under certain conditions, causes a hydrodynamic instability, yielding convective transport of the charge carriers or a convective current. This convective transport is here studied in the simplest case: namely, when the liquid layer is between two parallel plane electrodes, a distance d apart, and with injection of identical charge carriers (ions) on one electrode only. Earlier experimental observations in liquids, such as nitrobenzene, which have a viscosity and density almost like water showed that the observed current density was just a multiple of the current density due to the drift of the charge carriers, called mobility K, and apparently independent of the applied voltage ϕ_0. Consequently, it seemed possible to describe the phenomena simply by replacing the mobility with an apparent mobility, and without introducing any hydrodynamical equations (Atten & Gosse 1969). An expression for this apparent mobility was derived by Ostroumov (1954), Stuetzer (1962) and by Félici (1969). The latter called it *hydrodynamic mobility*, to point out its hydrodynamic, rather than electrochemical, origin. It was nevertheless puzzling that the current density ratio I/I_0 (called here the electric Nusselt number Ne) remained independent of the applied voltage, which is very much different from what is observed in the analogous thermal problem. Recent experiments, carried out in liquids of much higher viscosity, however, showed a definite dependence of Ne on the applied voltage (Hopfinger & Lacroix 1972). A more systematic study, which this called for, using liquids of very different viscosities and dielectric constants, revealed, indeed, a variation in Ne at sufficiently low values of ϕ_0, and a saturation in Ne at higher voltages. These experimental results are presented here; and a simple analysis of this rather original convection problem is proposed.

The instability study of the problem considered was carried out by Atten & Moreau (1972). The same instability problem, but with charge injection on a free surface, was solved by Schneider & Watson (1970). These studies show that the onset of instability is associated with a critical number (independent of d), which amounts to a critical voltage. Experimentally it is observed that, near the critical voltage, the motion has the structure of hexagonal cells. When the voltage is further increased, the motion eventually becomes turbulent. In the turbulent state, and probably before, the mean charge distribution is uniform in the core region. Since at the electrodes the velocity goes to zero, and continuity of the current requires that the bulk convective transport is matched by drift transport, the boundary regions must be characterized by strong gradients. A knowledge

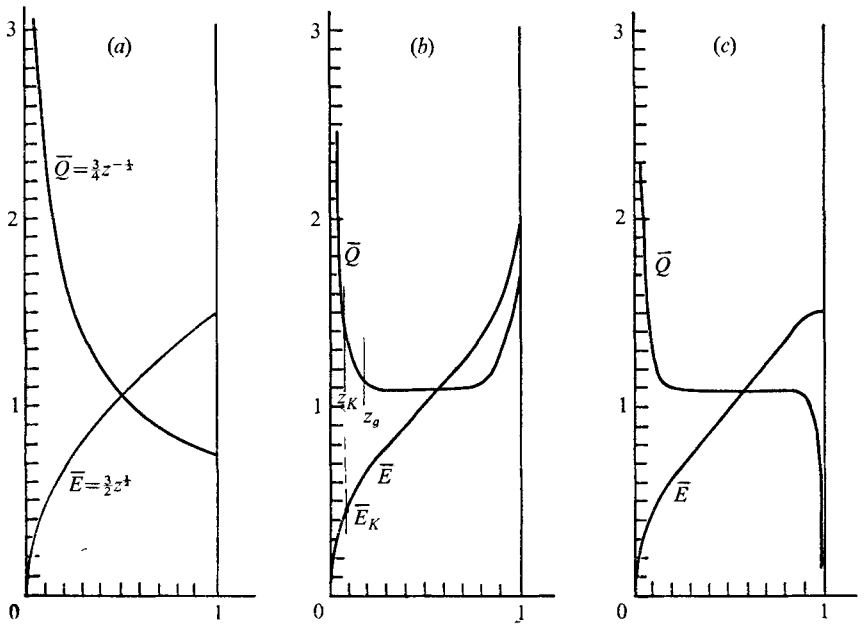

FIGURE 1. Representative distribution of mean charge and electric field: (*a*) no motion; (*b*) in turbulent state of motion without molecular diffusion; (*c*) turbulent state with molecular diffusion.

of the structure of these regions is thus important in understanding the steady-state convective transport of the charge carriers.

A first attempt to analyse the convective charge transport was made by Hopfinger & Gosse (1971). In this work, only the transient state was considered (i.e. the state established when a step voltage well above the critical value is suddenly applied, and a 'turbulent' layer appears near the injecting electrode, until the whole space between the electrodes is invaded by it). In this case, a strong mean charge gradient extends from the injector up to the interface between the turbulent and non-turbulent fluid, which justifies the assumption of a predominant gradient-type charge transport. The steady-state electrohydrodynamic convection problem is, although conceptually simpler, complicated, owing to the asymmetrical nature (see figure 1(*b*)) of the charge and electric field distributions, and the fact that the boundary conditions on the mean charge density are functions of the state of motion. Furthermore, the body force term is nonlinear. For these reasons, the experimental results are emphasized, and at this stage we content ourselves with a rather simple analysis, mainly in the hope of clarifying the physical phenomena.

2. Governing equations

The equations governing the problem are in non-dimensional form

$$\left(R\frac{\partial}{\partial t}-\nabla^2\right)u_i = -Ru_j\frac{\partial u_i}{\partial x_j}-R\frac{\partial p}{\partial x_i}+M^2RQE_i, \tag{1}$$

$$\frac{\partial Q}{\partial t} = -u_i\frac{\partial Q}{\partial x_i}-\frac{\partial (QE_i)}{\partial x_i}, \tag{2}$$

$$\frac{\partial u_i}{\partial x_i} = 0, \quad \frac{\partial E_i}{\partial x_i} = Q, \quad E_i = -\frac{\partial \phi}{\partial x_i}, \tag{3}$$

where $$x_i = x_i^*/d, \quad t = t^*K\phi_0/d^2, \quad u_i = u_i^*\,d/K\phi_0,$$
$$p = p^*d^2/\rho(K\phi_0)^2, \quad E_i = E_i^*\,d/\phi_0, \quad Q = Q^*d^2/\epsilon\phi_0, \quad \phi = \phi^*/\phi_0.$$

ϵ is the dielectric constant or permittivity of the fluid; ϕ the electric potential (ϕ_0 the applied voltage); Q the charge density and E the electric field. The other variables have their usual meaning. In (2) the diffusion term is neglected, since its contribution to the current density is small compared with the mobility current density. The characteristic parameters that appear are

$$M = \frac{1}{K}\left(\frac{\epsilon}{\rho}\right)^{\frac{1}{2}} \quad \text{and} \quad R = K\frac{\phi_0}{\nu}. \tag{4}$$

ρ is the density of the fluid; ν is the kinematic viscosity. It is the number $T = M^2R$ that plays the role of the Rayleigh number. Equations (1)–(3) result in the following equations for the mean charge distribution, the charge fluctuation and the velocity fluctuations, taking into account that, in the problem considered, $\bar{E}_i = \bar{E}(z)$ and $\overline{u}_i \equiv 0$:

$$\frac{d}{dz}(\bar{Q}\bar{E}) = -\frac{d\overline{wq}}{dz}, \tag{5}$$

$$\left(R\frac{\partial}{\partial t}-\nabla^2\right)u_i = -Ru_j\frac{\partial u_i}{\partial x_j}-R\frac{\partial p}{\partial x_i}+M^2R\bar{E}qk_i, \tag{6}$$

$$\frac{\partial q}{\partial t}+\bar{E}\frac{\partial q}{\partial z}+2\bar{Q}q = -w\frac{d\bar{Q}}{dz}-\left(u_i\frac{\partial q}{\partial x_i}-\overline{u_i\frac{\partial q}{\partial x_i}}\right). \tag{7}$$

The co-ordinate system is such that the plane of the electrodes is parallel to the x, y plane; and z is measured perpendicular to it, with the origin at the injecting electrode. Integration of (5) gives

$$\bar{Q}\bar{E}+\overline{wq} = I. \tag{8}$$

This is the non-dimensional current density $I = I^*d^3/K\epsilon\phi_0^2$. In (7) the term $w(d\bar{Q}/dz)$ represents production of charge fluctuations as usual, the term $2\bar{Q}q$ represents decay of charge fluctuations due to the Coulomb repulsion, and $\bar{E}(\partial q/\partial z)$ represents production or decay of charge fluctuations due to the drift of the charge. In (5)–(8), terms in the electric field fluctuation were neglected compared with terms in $\bar{E}$. This is justified in the core; but it may be questioned in the boundary regions. However, since $qe \leqslant \bar{Q}\bar{E}$, and since $\bar{Q}\bar{E}$ is a fraction of $\overline{wq}$, these terms never become very important.

The boundary conditions on the velocity field are the same as in the thermal problem. For the electrical variables we have

$$\phi(0) = 1, \quad \phi(1) = 0, \quad \bar{Q}(0) = \infty \Leftrightarrow \bar{E}(0) = 0. \tag{9}$$

$\bar{Q}(0) = \infty$ corresponds to the asymptotic case of space charge limited current, obtained when the injection is strong. Without motion, the electric field and charge distributions are in this case $E = \frac{3}{2}z^{\frac{1}{2}}$, $Q = \frac{3}{4}z^{-\frac{1}{2}}$, giving

$$I_0 = QE = \tfrac{9}{8}. \tag{10}$$

3. Classification of the mechanisms

Since molecular diffusion plays no role in the problem, on the boundaries the convective transport must be matched by drift transport. The ratio of molecular diffusivity to mobility is given by the Einstein relation $D/K = kT/e$. This means that molecular diffusion is limited to a region in which the potential drop is of the order of $\frac{1}{40}$ V. Neglecting diffusion has an important consequence on the mean charge distribution near the collector (as illustrated in figure 1). Experiments in a very viscous liquid have been carried out, to make the boundary regions accessible for measurements using the Kerr electro-optic effect. The experimental results (presented in § 8) show clearly that a structure similar to figure 1 (*b*) prevails. Convective transport is thus indeed matched by drift transport: any contribution of molecular diffusion would be within the region of predominant drift transport. It follows that a region near the receiving electrode exists where convective charge transport is against a relatively strong gradient of mean charge, a situation which to our knowledge has never been encountered before. Kraichnan's (1962) mixing-length analysis of thermal convection at arbitrary Prandtl numbers would seem to be well suited for a first analysis of the present problem, since the equivalent of the Prandtl number is $1/R$, which depends not only on the properties of the fluid, but also on the applied voltage, and consequently ranges in one experiment from small to large values. Indeed, such an analysis seemed to give good results (Hopfinger & Lacroix). But more extensive experimental investigations revealed that the essential parameter characterizing transition in the convection states is MR (equivalent to T/M), rather than R, which is an electric Reynolds number, related to an ordinary Reynolds number.

Thus, two asymptotic states are to be considered. One corresponds to MR small. This means that *viscosity dominates throughout* the space. In this case, there are two spatial regions of distinct charge-transport mechanisms. But it is convenient to consider the three regions: (i) $z < z_K$, dominant drift transport; (ii) $z_K < z \ll z_g$, dominant convective transport and strong gradient of mean charge; (iii) $z_g < z < \frac{1}{2}d$, dominant convective transport and weak gradient of mean charge. The other asymptotic state corresponds to high values of MR. This implies that *eddy viscosity is everywhere dominant*. The two regions in this state are (i) $z < z_g$, where strong gradients of mean charge exist; (ii) $z_g < z < \frac{1}{2}d$, weak mean charge gradient. Note that here $z_K \ll z_g$.

4. Analysis of the case of small MR

4.1. *Velocity distribution*

The analysis at low values of MR is based on two assumptions. (i) There exists a cellular or quasi-cellular motion, which can be characterized by a well-defined wavenumber. (ii) As the number T increases, the velocity field remains similar, so that

$$w(z) = Aw_0(z), \tag{11}$$

with $\max|w_0(z)| = 1$. Following Kraichnan's analysis, the thickness z_K could be defined by the condition that, at $z = z_K$, the convective charge transport represented by $\overline{wq}$ equals the mobility current $\bar{Q}\bar{E}$. A more meaningful definition in the present problem is that z_K specifies the distance from the electrode where the fluid velocity equals the ion velocity, i.e.

$$w(z_K) = \bar{E}(z_K) = \bar{E}_K.$$

This definition is motivated by the equations. For, when it is assumed that q and w are in phase ($\overline{wq} = wq$) we obtain from (5) and (7) (in which only the important terms are retained) equations for $\partial q/\partial z$ and $d\bar{Q}/dz$ in which these gradients are multiplied by $(w^2 - \bar{E}^2)$, showing the particularity of the point $z = z_K$. Furthermore, since at $z = z_K$ there may be locations where the fluid and ion velocity compensate each other, the charge density at these locations vanishes, which means that $q(z_K) \simeq \bar{Q}(z_K) = \bar{Q}_K$, and consequently

$$\overline{wq}(z_K) \simeq \bar{E}_K \bar{Q}_K. \tag{12}$$

From the boundary conditions on the electrode ($w(0) = \partial w/\partial z(0) = 0$), it follows that close to the electrodes the velocity distribution is quadratic, so that when z_K is small enough $w(z)$ can be written as

$$w(z) = Aw_0(z) \simeq A\lambda z^2, \quad z \leqslant z_K. \tag{13}$$

4.2. *Expression for the current density*

In the vicinity of the injector, the convection current is negligible (i.e. $I = \bar{Q}\bar{E}$); consequently, $\bar{E}(z) = az^{\frac{1}{2}}$ and $\bar{Q}(z) = \frac{1}{2}az^{-\frac{1}{2}}$. At $z = z_K$, the convection influences $\bar{Q}$ appreciably, but $\bar{E}$ very little. Thus $\bar{E}_K \simeq az_K^{\frac{1}{2}}$, and

$$\bar{Q}_K \simeq I/2\bar{E}_K \simeq \bar{E}_K/4z_K. \tag{14}$$

Equation (7) in this spatial region may be written as

$$\bar{E}\frac{\partial q}{\partial z} + 2\bar{Q}q \simeq -w\frac{d\bar{Q}}{dz}. \tag{15}$$

Substituting in (15) for $\bar{E} = az^{\frac{1}{2}}$ and $\bar{Q} = \frac{1}{2}az^{-\frac{1}{2}}$, and integrating it, gives

$$q(z) \sim \tfrac{1}{2}\bar{Q}_K z/z_K, \quad z \leqslant z_K.$$

Owing to the approximation to $\bar{Q}$, q is under-estimated; this is not inconsistent with $q(z_K) \simeq \bar{Q}_K$. The latter relation, together with (12)–(14), yields an expression for the current density in the form

$$I \simeq \tfrac{1}{2}\bar{E}_K^{\frac{3}{2}}\lambda^{\frac{1}{2}}A^{\frac{1}{2}}. \tag{16}$$

4.3. *Evaluation of* E_K

In the thermal problem, the analysis of the boundary layers gives the expected expression for the heat flux, because the temperature variation is confined to the boundary layers. In the problem considered, the electric potential drops throughout the space, including the core. It is therefore necessary to analyse all the regions. In regions (ii) and (iii), the fluid velocity is higher than the ionic velocity; one might expect return columns of charge-free liquid, indicating that $q \sim \bar{Q}$. This is verified by an order-of-magnitude analysis of (6) and (7), which are moreover satisfied by $\bar{Q} \propto z^{-1}$. Then we can approximate q and $\bar{Q}$ in region (ii) by

$$q \simeq \bar{Q} = \bar{Q}_K z_K / z.$$

In region (iii), characterized by a weak gradient of $\bar{Q}$, q and $\bar{Q}$ are approximated by

$$q(z) = \bar{Q}(z) = \bar{Q}(\tfrac{1}{2}) = \frac{I}{\bar{E}(\tfrac{1}{2}) + w(\tfrac{1}{2})} \simeq \frac{I}{1+A}.$$

The boundary z_g between the two regions is such that

$$z_g = \bar{Q}_K z_K (1+A)/I.$$

Integration of Poisson's equation $d\bar{E}/dz = \bar{Q}$ between z_K and $\frac{1}{2}$, using successively the two above expressions for $\bar{Q}$, subject to the approximate condition $E(\frac{1}{2}) = 1$, gives, after some rearrangement,

$$\bar{E}_K = 1 - \frac{\lambda^{\frac{1}{2}}}{4} \frac{\bar{E}_K^{\frac{3}{2}} A^{\frac{1}{2}}}{1+A} + \frac{\bar{E}_K}{4}\left[1 + \log \frac{2\bar{E}_K}{1+A}\right]. \tag{17}$$

A plausible approximation of $w_0(z)$ is $16z^2(1-z)^2$, which leads to $\lambda = 16$. With this value of λ, $\bar{E}_K$ remains constant within 2 % when A varies from 1 to 15 ($\bar{E}_K \simeq 0{\cdot}8$). But the validity of (17) is limited by the condition $z_g \leqslant \frac{1}{2}$, which gives $A \leqslant 12$. This analysis leads to the conclusion that the electric field at $z = z_K$ is practically independent of the velocity norm A, and consequently the mobility-dominated layer is characterized by a constant field drop (since $E(0) = 0$). Equation (16) can then be written as $I \simeq 1{\cdot}4A^{\frac{1}{2}}$. This finally gives the electric Nusselt number

$$Ne = I/I_0 = \tfrac{8}{9} I \simeq 1{\cdot}2A^{\frac{1}{2}}. \tag{18}$$

4.4. *Relation between* A *and* T

The relation between A and T is obtained from (6), in which the inertial terms are neglected, and which, when multiplied by u_i and integrated from 0 to 1, gives

$$\int_0^1 \overline{u_i \nabla^2 u_i}\, dz = \int_0^1 \overline{u_i \frac{\partial p}{\partial x_i}}\, dz + T \int_0^1 \bar{E}\overline{qw}\, dz.$$

By the similarity assumption for the velocity distribution, the left-hand side is proportional to A^2. The first integral on the right-hand side vanishes, and the second integral can be written as

$$\int_0^1 \bar{E}\overline{qw}\, dz = \int_0^{z_K} \bar{E}\overline{qw}\, dz + \int_{z_K}^{1-z'_K} \bar{E}\overline{qw}\, dz + \int_{1-z'_K}^{1} \bar{E}\,\overline{qw}\, dz.$$

z'_K specifies the thickness of the mobility-dominated layer on the collector. Since, in the mobility-dominated layers, the convection may be neglected, the only integral left is the second on the right-hand side. This can be approximated by

$$TA\int_{z_K}^{1-z'_K}\bar{E}(z)\,w_0(z)\,q(z)\,dz \simeq \tfrac{1}{2}TA\int_{z_K}^{1-z'_K} w_0(z)\,\frac{d\bar{E}^2}{dz}\,dz.$$

$q(z) \simeq \bar{Q}(z) = d\bar{E}/dz(z)$ has been used, which is valid in regions (ii) and (iii). If z_K and z'_K are sufficiently small, the gradient dE^2/dz is practically independent of A, and the integral is practically a constant, giving

$$A \sim T. \tag{19}$$

The expression for Ne can finally be written in the form

$$Ne \sim T^{\frac{1}{2}} \quad \text{for } MR \text{ small.} \tag{20}$$

5. Analysis for high MR values

5.1. *z dependence of the quantities in region* (i)

Here the number T is considered to be high enough to justify the assumption that the eddy viscosity is dominant everywhere. The boundary layers are assumed to be in turbulent motion, and the laminar sublayer as well as the mobility dominated sublayer are neglected.

Unipolar injection into nitrobenzene under high voltage is characterized by a quasi-linear electric field distribution in the core, and consequently by a nearly constant distribution of mean space charge density. This is attributed to the efficient mixing property of turbulence. As the space charge density on the injecting electrode is very high, this observation is evidence for the existence of a boundary layer with a strong mean charge gradient defined as region I. The production of charge fluctuations is associated with $d\bar{Q}/dz$. Therefore it is confined to this region. An order-of-magnitude analysis of (7)

$$|w'\,d\bar{Q}/dz| \sim |w'\,dq'/dz| \tag{21}$$

(where w' denotes the root-mean-square z component of the fluctuating velocity field), and of (6)

$$|w'\,dw'/dz| \sim M^2\bar{E}q', \tag{22}$$

taking into account (5), leads to the following expressions for the z dependence of w', q', $\bar{E}$ and $\bar{Q}$:

$$w' \propto z^{\frac{1}{2}}, \quad q' \propto z^{-\frac{1}{2}},$$
$$\bar{E} \propto z^{\frac{1}{2}}, \quad \bar{Q} \propto z^{-\frac{1}{2}}.$$

These are valid in region (i). The variations of $\bar{E}$ and $\bar{Q}$ in this region are thus identical to the variations of E and Q in the state of no motion.

5.2. *Relation between w' and E*

The relation between the root-mean-square value of the fluid velocity and the electric field is crucial for the calculation of the current. An energy argument (used by Veronis (1966), in the case of the thermal problem) gives us an upper

bound for w'. Since we consider here the turbulent state, we may assume that the electric charge is transported by blobs of fluid moving away from the injector, and the kinetic energy is here generated by a conversion of the electrostatic energy. Between the injector and the outer region of the charge boundary layer (region of strong $\bar{Q}$ variation), the electric field varies from zero to $\bar{E}(z_g)$. The electrostatic energy in a blob which extends from the injector up to z_g can be evaluated as $\mathscr{E} \leqslant \frac{1}{2}\epsilon\bar{E}^2(z_g)$. It may be assumed that this energy is completely converted to kinetic energy with a predominance in the w' component. We then have

$$\tfrac{1}{2}\rho w'^2 \leqslant \tfrac{1}{2}\epsilon\bar{E}^2(z_g) \quad \text{or} \quad w' \leqslant (\epsilon/\rho)^{\frac{1}{2}}\bar{E}(z_g).$$

In non-dimensional form this gives

$$w' \leqslant M\bar{E}(z_g). \tag{23}$$

This energy argument is implicit in (21). If it is assumed that $q' \leqslant \bar{Q}$, this equation can be written as

$$\frac{dw'^2}{dz} \leqslant M^2\frac{d\bar{E}^2}{dz},$$

which gives (23) with $\bar{E} = w' = 0$ at $z = 0$.

5.3. *Expression for the current density*

To obtain the expression for the current density, it is necessary to take into account the core in which $d\bar{Q}/dz$ takes low values. As already pointed out, the production of charge density fluctuations in this region is negligible, so that q' is a decreasing function of z (Coulomb and eddy damping). The vorticity production on the contrary is not confined to region (i). It decreases like $\bar{E}q'$, so that the variations of w' with z are not very important.

Let us consider now a point of abscissa $z_1 \ll 1$ in the core, such that

$$\frac{d\bar{Q}}{dz}(z_1) \simeq 0.$$

At $z = z_1$, the relation $w' \sim ME$ is still valid (in order of magnitude) but $q' \sim Q$ is not. To evaluate the ratio $q'/\bar{Q}$, let us use the current continuity equation (5):

$$\frac{d}{dz}(\bar{Q}\bar{E}) \simeq \bar{Q}^2 \simeq \left|\frac{d}{dz}(q'w')\right|. \tag{24}$$

From (22) and (23), we deduce

$$|dw'/dz| \sim Mq'.$$

The main terms in (7) give the balance (for the core)

$$\bar{Q}q' \sim |w'\,dq'/dz|;$$

and (24) leads to

$$\bar{Q}^2 \sim Mq'^2 + \bar{Q}q'.$$

For M values significantly higher than 1, we obtain

$$q'/\bar{Q} \sim M^{-\frac{1}{2}}. \tag{25}$$

Putting $w'(z_1) \simeq \gamma M \bar{E}(z_1)$ and $q'(z_1) \simeq \delta M^{-\frac{1}{2}} \bar{Q}(z_1)$, the current density is

$$I = \bar{Q}\bar{E} + \overline{qw} \simeq \bar{Q}\bar{E} + \alpha q' w' \simeq \bar{Q}\bar{E}(z_1)\,[1 + \beta M^{\frac{1}{2}}], \tag{26}$$

with $\beta = \alpha\gamma\delta$. ($\alpha$ is the mean correlation coefficient of the velocity and charge density fluctuations: here $\alpha \simeq \frac{1}{2}$.)

If the mean charge density can be approximated by $\bar{Q} = \text{const.}$, the mean electric field is

$$\bar{E}(z) = 1 - \tfrac{1}{2}\bar{Q} + \bar{Q}z.$$

The electric Nusselt number is then ($z_1 \ll \frac{1}{2}$), given by

$$Ne = \frac{I}{I_0} = \frac{8I}{9} \simeq \frac{8}{9}\bar{Q}(1 - \tfrac{1}{2}\bar{Q})\,(1 + \beta M^{\frac{1}{2}}). \tag{27}$$

In the thermal convection problem the principle of maximum dissipation, equivalent to a maximum heat flux, has led to good results (Malkus 1954; Spiegel 1962). In the present problem it is seen from (27) that Ne is a maximum for $\bar{Q} = 1$. This yields

$$Ne \simeq \tfrac{4}{9}(1 + \beta M^{\frac{1}{2}}). \tag{28}$$

Expression (28) states that Ne is independent of T or R, which reflects the saturation observed previously. Since β is of order 1, we can conclude that, at high values of M, the Nusselt number varies as $M^{\frac{1}{2}}$.

6. Transition in the states of convection

The character of the relevant transition number can be obtained by simply equating the expressions for Ne in both regions,

$$C_1 T^{\frac{1}{2}} \simeq C_2 M^{\frac{1}{2}},$$

giving

$$MR \simeq \text{const.}$$

This is evidence that transition is indeed characterized by a number MR, which is an electric Reynolds number.

Since transition is due to a change from a viscous to a nonlinear flow regime, at the transition the viscous terms in (6) will be of the same order as the inertial terms, i.e.

$$|\nabla^2 u_i| \sim R|u_j\, \partial u_i/\partial x_j|.$$

A pseudo-cellular model (as employed by Kraichnan) would give a Reynolds number of order π. Moore & Weiss (1973) indicate that the analogous thermal transition from viscous to nonlinear flow occurs at a Reynolds number $Re_T \simeq 10$. When taking this value as the transition value, we can write in the viscous approximation

$$Re_T = RA_T = 10.$$

From (19) we have $A \sim T$; and a more precise expression is

$$A \simeq T/T_c. \tag{29}$$

Such an expression has been obtained by Félici in the case of weak injection. Also, Atten & Lacroix (1974) have shown that at the onset of instability the

Liquid and injected ions	Dielectric constant ϵ	Density ρ (g cm^{-3})	Viscosity η (cP)	Mobility K (cm^2(V s)$^{-1}$)	$M = \frac{1}{K}\left(\frac{\epsilon}{\rho}\right)^{\frac{1}{2}}$	Critical voltage ϕ_c (V)	Critical number $(T_c)_{exp}$
Methanol H^+	33·5	0·80	0·60	$1{\cdot}47 \times 10^{-3}$	4·1	—	—
Chlorobenzene Cl^-	6	1·1	0·8	$4{\cdot}5 \times 10^{-4}$	4·9	60	88
Ethanol H^+	25	0·785	1·1	6×10^{-4}	8·8	25	84
Cl^-				2×10^{-4}	26·5	—	—
Nitrobenzene Cl^-	35	1·2	1·6	$2{\cdot}3 \times 10^{-4}$	22	11	92
Propylene carbonate Cl^-	69	1·2	2·48	$1{\cdot}4 \times 10^{-4}$	51	5	88
Pyralene 1460 Cl^-	5·9	1·41	10	$3{\cdot}2(\pm 0{\cdot}2) \times 10^{-5}$	60	50	82
Pyralene 1500 Cl^- 20 °C	6·4	1·35	50	$7(\pm 0{\cdot}5) \times 10^{-6}$	292	50	81
35 °C	6·1	1·34	20	$1{\cdot}6(\pm 0{\cdot}1) \times 10^{-5}$	126	50	83
Pyralene 1499 Cl^-	5·6	1·38	90	$4(\pm 0{\cdot}5) \times 10^{-6}$	475	55	76

TABLE 1. Physical constants characterizing the liquids studied and the injected ions at the temperature $\theta = 20$ °C, and values of the voltage for which the instability sets in (unipolar injection)

possible stable laminar motion is characterized by a maximum fluid velocity higher than the ionic velocity. (A value of $A \simeq 1{\cdot}2$ was obtained, with $\bar{Q}(0) = 10$.) With (29) we get

$$RA_T \simeq \frac{(RT)_T}{T_c} = \frac{(MR)_T^2}{T_c} \simeq 10 \quad \text{or} \quad (MR)_T \simeq (10T_c)^{\frac{1}{2}}.$$

When taking the experimental value of $T_c \simeq 90$ (see table 1), we obtain

$$(MR)_T \simeq 30.$$

The same value must naturally be obtained when extrapolating the turbulent or high MR approximation. In this state, the Reynolds number may be expressed by

$$Re \simeq R \max(w'(z)).$$

The foregoing analysis has shown that, in region (i), $w' \sim M\bar{E}$, and that w' decreases with z in the core. With $\bar{Q} = 1$ in the core, we get for the velocity maximum

$$\max w'(z) = bM\bar{E}(z_1) \simeq \tfrac{1}{2}bM.$$

Hence, from $Re = 10$, $$(RM)_T \simeq 20/b.$$

For the two numerical values of $(MR)_T$ to be equal, we must have $b \simeq \frac{2}{3}$, which in turn gives for the velocity $\max w'(z) \simeq \frac{1}{3}M$. This shows a saturation in the non-dimensional velocity.

7. Experimental apparatus and procedures

7.1. *Test cell*

The experimental apparatus used for this study is very similar to that used in previous studies (Atten & Gosse 1969; Lacroix & Tobazéon 1972). The test cell is a Teflon unit containing two circular plane metal† electrodes (32 mm in diameter), which are covered with ion exchange membranes. The gap between the electrodes can be varied between 0 and 1 cm. The membranes (AMF 60) are anionic or cationic, depending on the polarity of the ions to be injected. One serves as injector, the other as collector. With these composite electrodes, a strong and reproducible injection of known ions into polar liquids is achieved. The test cell has two optical windows, through which the electric field distribution is measured by the electro-optic Kerr method and the liquid motion is observed by the schlieren method.

7.2. *Purification circuit*

The commercially available dielectric liquids have a residual conduction either due to the presence of electrolytic impurities (which are more or less dissociated, depending on the dielectric constant of the liquid), or possibly due to an auto-dissociation of the liquid itself, as is the case for ethanol. To study the phenomena due to unipolar injection only, it is necessary to reduce this residual conduction, so that it becomes negligible as compared with the current due to the ion injection.

† For some of the schlieren observations, metal plated and varnished glass electrodes were used.

A sufficient purification is obtained by circulating the liquid periodically through a purification circuit, which contains an ion purification cell, preceded by a chemical purification system. The test cell is part of this circuit; but it is isolated from it during the measurements, simply by closing some stopcocks. This circuit also contains a heat exchanger, which allows one to keep the temperature constant throughout the measurements.

7.3. *Choice of the electrode separation*

The stability criteria, as well as the variation of the electric Nusselt number, do not depend on the thickness of the liquid layer. (Note that, on the contrary, the Rayleigh number depends on d.) But it is necessary to vary d in the experiments, for the following reasons. The range of values of the applied voltages is specified by the instability criterion, and by the value of the electric Reynolds number, which characterizes transition from the viscous to the inertially dominated state of motion. For the most viscous liquids, this may require voltages ranging from a few volts to tens of kilovolts. Since the residual conduction current in the ohmic range is $\sigma\phi_0/d$ (σ is the conductivity of the liquid), and the injection current is roughly $K\epsilon\phi_0^2/d^3$, it is necessary to keep, at small values of ϕ_0, the distance as small as possible, for the injection current to remain dominant. But the geometrical imperfections of the membranes impose that $d > 0{\cdot}1$ mm. On the other hand, at high voltages, a large gap must be chosen, so that the field strength remains below the value that causes a breakdown of the liquid.

7.4. *Electro-optic Kerr method*

The electric field distribution is measured using the Kerr electro-optic effect. Figure 2 shows a schema of the optical arrangement used. Under the influence of the electric field, the liquid behaves like a uni-axial birefringent crystalline plate, which has one of the principal axes aligned with the electric field. The optical phase shift is given by $\delta = 2\pi B\Lambda E^2$. ($\Lambda$ is the optical path length, and B the Kerr constant of the liquid.) The monochromatic linearly polarized light beam used has a plane of polarization whose angle is at 45° with respect to the direction of the electric field, and it emerges from the cell elliptically polarized. The degree of elliptical polarization is measured by means of an analyser rotating at constant speed and a photo-detector (Budde 1962). The instrumentation makes it possible to measure directly the absolute value of $\cos\delta$. The light source is a helium–neon laser; and an optical system gives a light beam in the cell about 0·1 mm in diameter, and consequently permits measurements very close to the electrode.

8. Experimental results

Table 1 lists the physical properties of the liquids used in this study. The viscosity ranges from 0·6 to 90 centipoise, and the relative dielectric constant from about 6 to 69. The mobility values of the injected ions in the liquids used, obtained by conductimetry, are given in the literature, except for the pyralenes.†

† The French products named pyralenes are chlorinated diphenyls. In English-speaking countries their trade name is Aroclor.

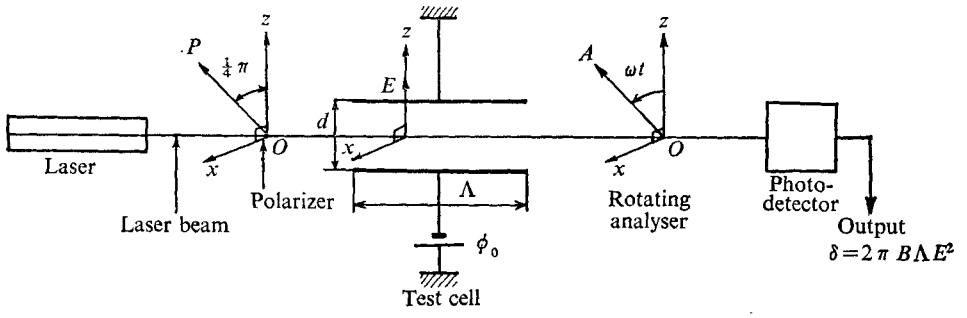

FIGURE 2. Schema of the Kerr electro-optic arrangement. OP, principal direction of the polarizer; OA, principal direction of the rotating analyser; Oz, direction of the electric field.

For the latter liquids the mobilities have been measured in this work both by conductimetry and by the time of the passage of the ions from the injector to the collector when a step voltage is suddenly applied. The value of the step is lower than the critical voltage.

8.1. *Variations of the current density*

For all the liquids studied the variation of the steady-state current density as a function of the applied voltage has been measured for various gap widths. All of them exhibit the same transition, verifying the independence of the phenomena of the gap width. The observations are illustrated for one liquid: namely, pyralene 1460.

In figures 3 and 4, the steady-state current density is plotted, respectively, as a function of the applied voltage for a fixed d, and as function of the gap width for a fixed voltage. These graphs show three states of charge transport. For applied voltages smaller than the critical value $\phi_c \simeq 50\,\mathrm{V}$, the current varies as ϕ_0^2/d^3. At values somewhat above ϕ_c, it varies like $\phi_0^{\frac{5}{2}}/d^3$; and at values above $\phi_T \simeq 1000\,\mathrm{V}$, the current varies again, as in the motionless state, like ϕ_0^2/d^3. But the schlieren observations show that, at these voltages, the liquid is very agitated, and that it is probably turbulent.

It should be noted that, for the liquid tested, the onset of instability can be determined only for small gap widths ($d \leqslant 0{\cdot}4\,\mathrm{mm}$), for which the residual current is sufficiently small. (For certain liquids, e.g. ethanol and methanol, this residual current cannot be made small enough, owing to the practical lower bound for d, so it was not possible to determine ϕ_c from the measurement of the steady-state current.) The transition value, conversely, is determined with large gaps (see § 7.3). The value $\phi_c \simeq 50\,\mathrm{V}$ was not deduced from figure 3, but from a more detailed study of I against ϕ_0 near ϕ_c. We may also point out that this electrical determination is at least as reliable as the deduction of ϕ_c from optical measurements (see § 8.3).

In general, the current is a function of the parameters M, R and $\bar{Q}(0)$, and it can be written in the form $I = (K\epsilon\phi_0^2/d^3) f(M, R, \bar{Q}(0))$.

Only the number $\bar{Q}(0)$ may be a function of the gap width ($\bar{Q}(0) = Q^*(0)\, d^2/\epsilon\phi_0$). Since the experimental observations show that the function f is independent of d,

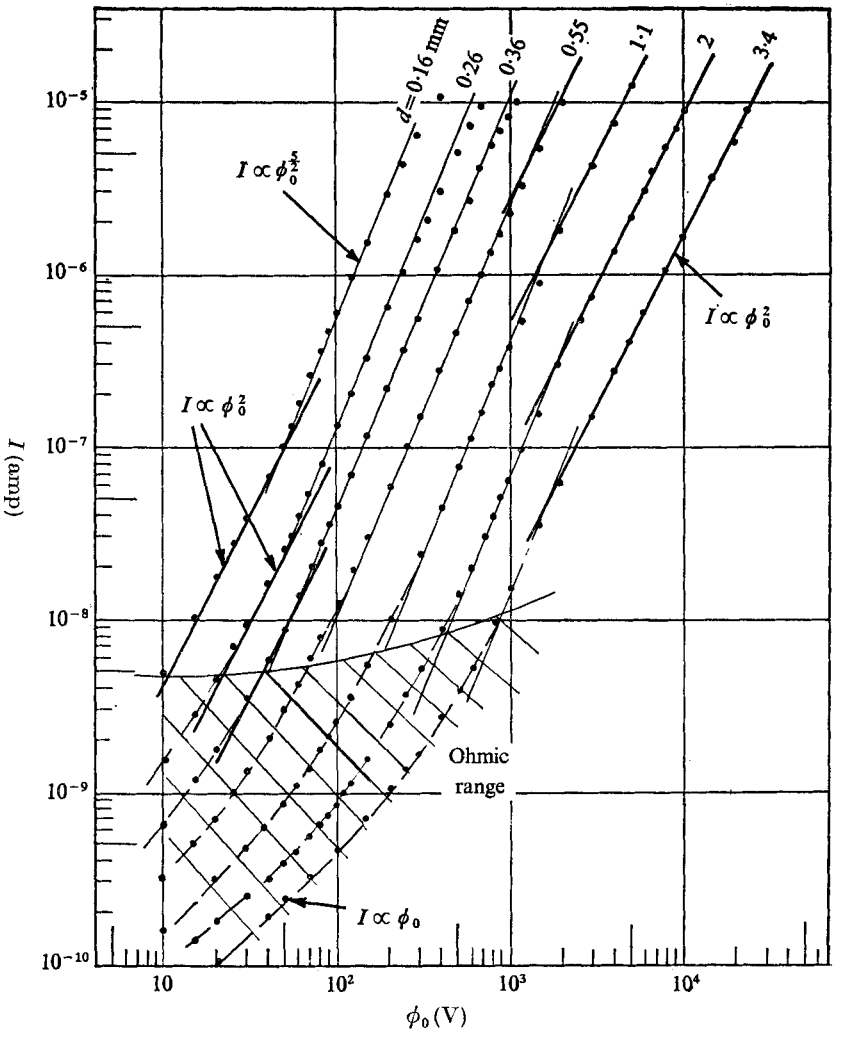

FIGURE 3. Variations of the electric current with applied voltage for fixed gap widths. The dotted branches of the curves, whose slope approaches one at low current densities, correspond to the ohmic range (the electrode surface is 8 cm²).

I must be independent of $\bar{Q}(0)$, which means that $\bar{Q}(0)$ is either constant or high. Since, at values of $\phi_0 < \phi_c$, it was found that $\bar{Q}(0)$ is higher than the value necessary for the assumption of space charge limited current to be valid, it can be concluded that $\bar{Q}(0)$ is always high. This is of importance for the validity of the established Nusselt number variations.

8.2. *Electric Nusselt number and transition*

In figure 5 the measured current densities in pyralene 1460 are presented in the form of an electric Nusselt number. By definition, this number has a value of 1 when $\phi_0 < \phi_c$; and, in accordance with the observed current densities, Ne varies like $\phi^{\frac{1}{2}}$ for values of $\phi < \phi_T$, and is a constant afterwards, indicating saturation.

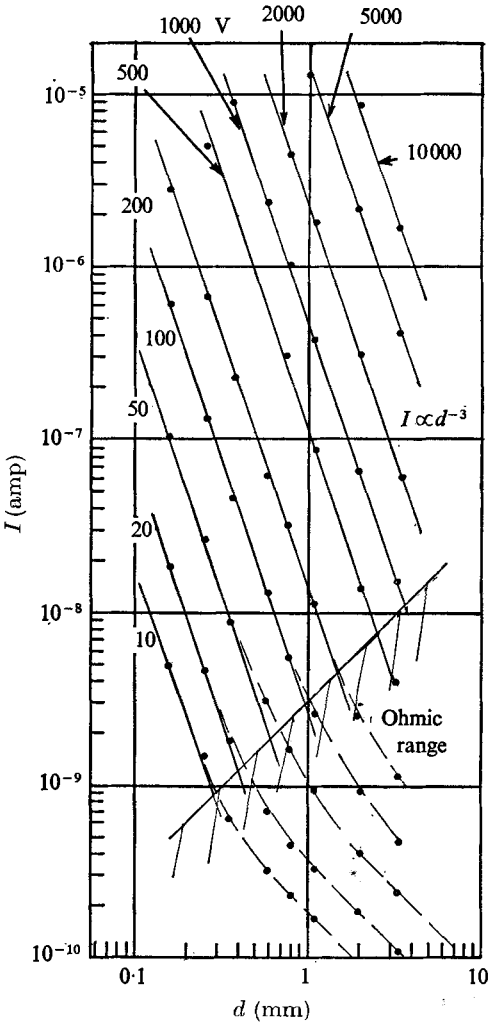

FIGURE 4. Variations of the electric current with gap width for fixed applied voltages. The dotted branches of the curves correspond to the ohmic range.

The results obtained for all the liquids are shown in figure 6, where the Nusselt number is presented as a function of $T/(T_c)_{\exp}$. As is predicted by the theoretical analysis, all the liquids have the same branch $Ne = (T/T_c)^{\frac{1}{2}}$. The saturation value of Ne depends on the physical properties of the liquid, and somewhat on the nature of the injected ions. If this saturation value Ne_s is plotted as a function of M (figure 7), the expression

$$Ne_s = (I/I_0)_s = (\tfrac{1}{3}M)^{\frac{1}{2}}, \quad M > 4,$$

can be deduced. This is in reasonably good agreement with the theoretical predictions.

The transition from the viscosity dominated hydrodynamic state to the inertially dominated state is gradual, so, at a certain applied voltage, the viscous

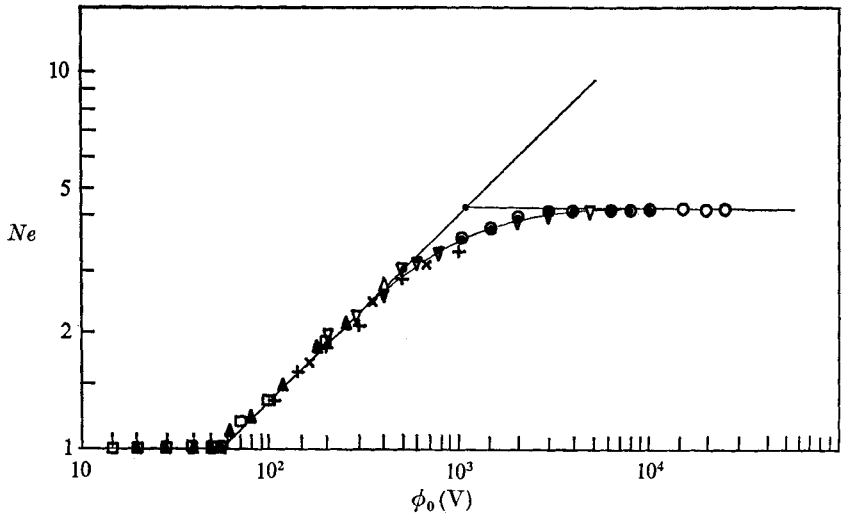

FIGURE 5. Electric Nusselt number variations with applied voltage in pyralene 1460.

	○	●	▽	+	×	△	□
d (mm)	3·4	2	1·1	0·55	0·36	0·26	0·16

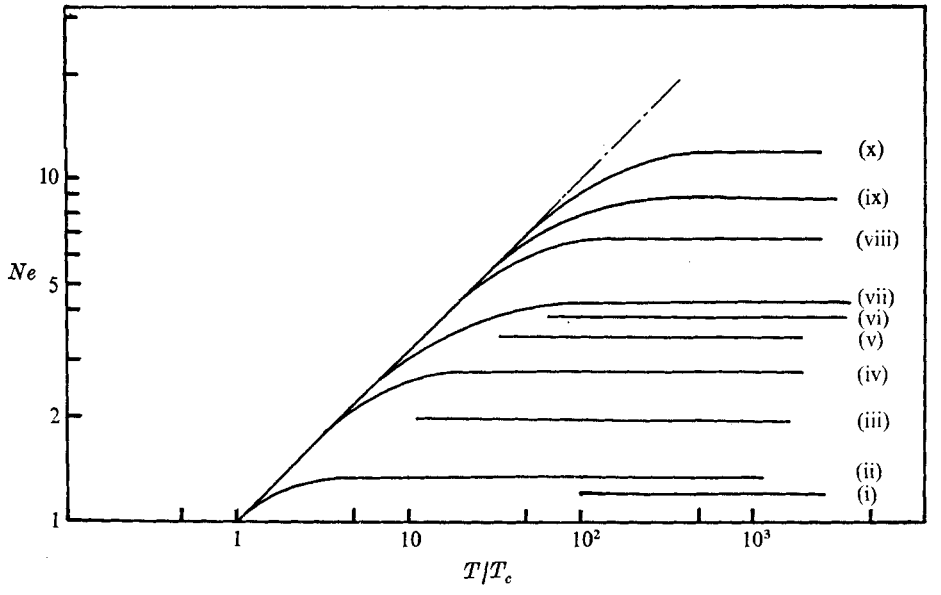

FIGURE 6. Electric Nusselt number versus the stability parameter $T/(T_c)_{exp}$ in different liquids: (i) methanol (H^+); (ii) chlorobenzene (Cl^-); (iii) ethanol (H^+); (iv) nitrobenzene (Cl^-); (v) ethanol (Cl^-); (vi) propylene carbonate (Cl^-); (vii) pyralene 1460 (Cl^-); (viii) pyralene 1500, 35 °C (Cl^-); (ix) pyralene 1500, 20 °C (Cl^-); (x) pyralene 1499 (Cl^-).

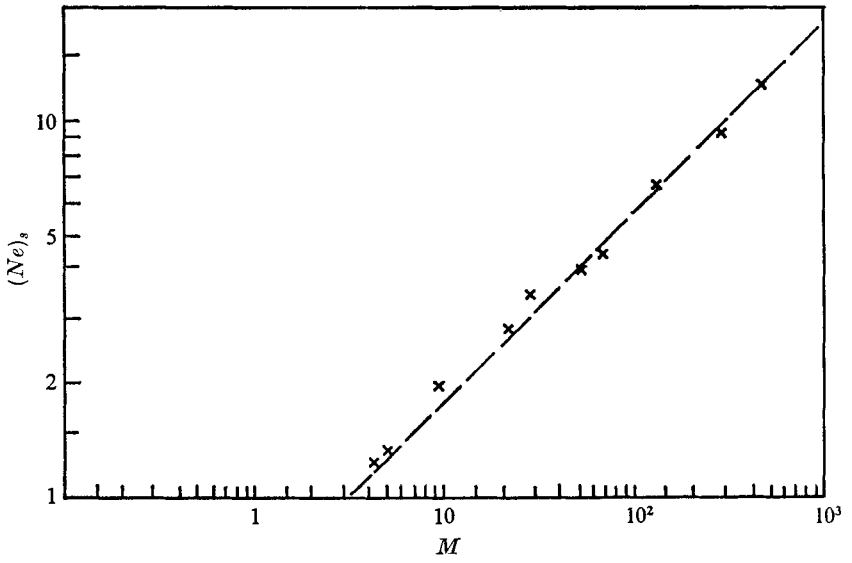

FIGURE 7. Saturation value of the electric Nusselt number as a function of the parameter M.

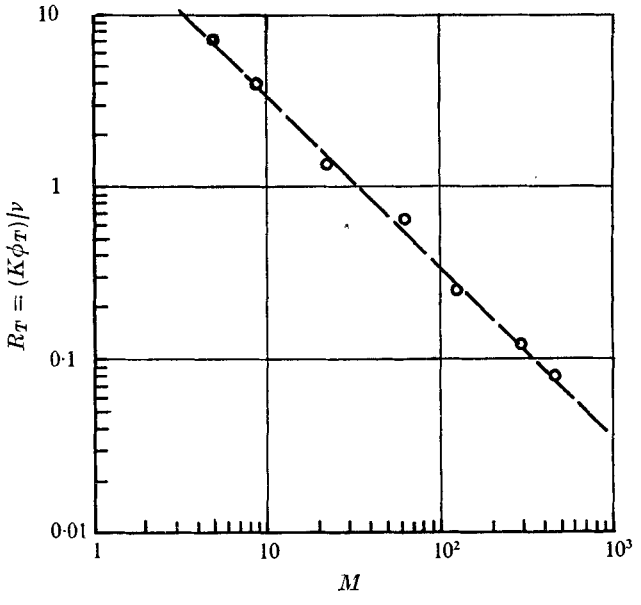

FIGURE 8. Dependence of the transition value $R_T = K\phi_T/\nu$ on M.

and inertial terms will be of the same order. The transition potential ϕ_T is defined by the intersection of the two branches of the curve $Ne = f(T, M)$ (i.e. the intersection between $Ne = (T/T_c)^{\frac{1}{2}}$ and $Ne = (\frac{1}{3}M)^{\frac{1}{2}}$), which yields

$$(MR)_T = \tfrac{1}{3}T_c \simeq 30.$$

This value is confirmed by figure 8, where $R_T = \phi_T K/\nu$ is plotted as a function of M.

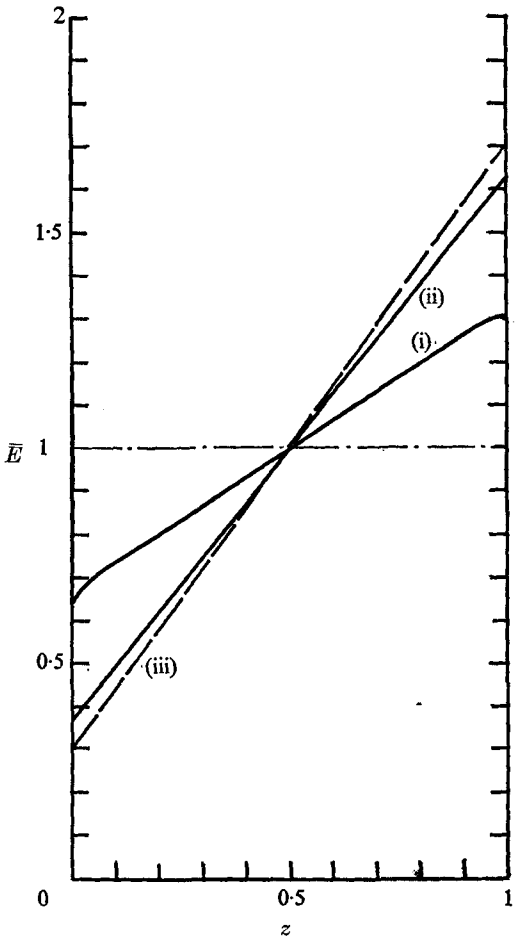

FIGURE 11. Electric field distribution in liquids of low viscosity.

	ϕ_0 (kV)	d (mm)
(i) Chlorobenzene	20	2
(ii) Nitrobenzene	20	4
(iii) Propylene carbonate	18	4

8.3. *Schlieren observations near* ϕ_c

Schlieren observations made in pyralenes 1460 and 1500 near the critical voltage confirmed that the change in the slope of the current density from ϕ_0^2/d^3 to $\phi_0^{\frac{5}{2}}/d^3$ corresponds to the onset of instability. These observations were made at small gap widths (0·1–0·7 mm), and with transparent electrodes, consisting of glass plates onto which a conducting layer (silver or indium oxide) was deposited. A varnish was then applied, which has properties similar to the ion exchange membranes (Félici & Sauviat 1972). At voltages below ϕ_c the liquid remains motionless, whereas, just above ϕ_c, very stable hexagonal cells are established (see figure 9, plate 1), a structure well known as Bénard cells in the thermal problem. The width of these cells is about twice the thickness of the liquid layer. When the

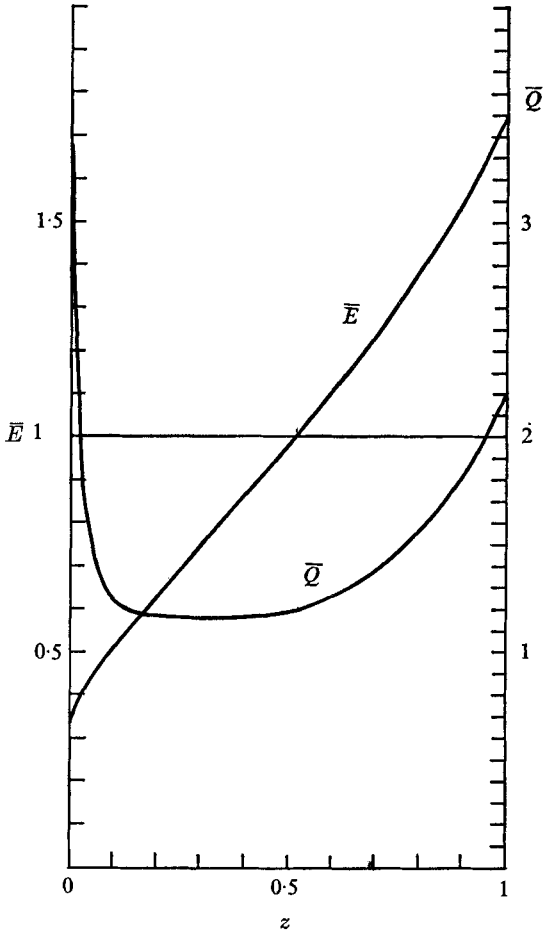

FIGURE 12. Electric field and charge density distribution in pyralene 1500. $\eta = 51$ cP; $d = 8$ mm; $\phi_0 = 25$ kV.

applied voltage is further increased up to 2–3 times ϕ_c, this cellular structure is progressively replaced by unsteady filaments (figure 10, plate 1). Such a quasi-cellular structure has already been observed between a rigid electrode and a free surface (Avsec & Luntz 1937; Schneider & Watson 1970).

8.4. *Electric field distribution*

Considering the value of the Kerr constant and the optical path length $\Lambda = 32$ mm, a measurable phase shift δ is obtained only at sufficiently high applied voltages (corresponding generally to more than 10 kV cm^{-1}). Also, since no reliable measurements can be carried out in a gap < 1 mm, it is not possible to measure the electric field distribution in the state $Ne \propto T^{\frac{1}{2}}$. So, for liquids of low viscosity, the measurements can be carried out only in conditions such that $MR \gg (MR)_T$. The observed distribution of the electric field in this case is apparently linear throughout (figure 11); the boundary layers are not even visible. The non-

dimensional mean charge density deduced from these field distributions is independent of the applied voltage and the gap width; and it has a value of 1·2–1·3 in nitrobenzene, propylene carbonate and pyralene 1460. This value is close to the value 1, deduced from the maximization of the current employed in § 5. In chlorobenzene, the field distribution is also linear, indicating that turbulence makes the charge uniform. But the mean charge density is only 0·7. This can be explained by the small value of M.

In liquids of high viscosity, like the pyralenes 1500 and 1499, the measured field distribution corresponds to values of MR of only a few times $(MR)_T$. In this case, boundary layers are clearly visible on the collecting electrode as well as on the injecting electrode (figure 12). On this curve, three zones can be distinguished: the boundary layer on the injector, where the mean charge density falls off rapidly; a core, where $\bar{Q}$ remains practically constant and its value is of order 1 ($\bar{Q} \simeq 1{\cdot}2$); and a boundary layer on the collector, where $\bar{Q}$ increases again. Taking figure 12 as an example, the value of the mean charge evaluated from the measured field distribution at a distance of about 0·1 mm from the electrode is 3·4, and the corresponding current due to the mobility (i.e. $\bar{Q}\bar{E}$) is only 15 % of the total current. From continuity of the current, it follows that, on the electrode, $\bar{Q}$ approaches very high values, which verifies the hypothesis of space charge limited injection ($\bar{Q}(0) = \infty$).

When the square of the electric field is plotted as a function of z (z measured from the electrode), a linear variation is indeed obtained in a region whose upper bound z is z_1. This behaviour is in agreement with the prediction that followed from the order-of-magnitude analysis of the governing equations (§ 5). The currents, due to convection and mobility, thus remain in constant proportions in this region, the latter being small, however. By varying the applied potential and the gap width systematically, it was possible to show that z_1 varied as $\nu d/\phi_0$. The Reynolds number associated with z_1, assuming that the velocity is given by $(\epsilon/\rho)^{\frac{1}{2}}\bar{E}(z_1)$, is

$$Re\,(z_1) \simeq (\epsilon/\rho)^{\frac{1}{2}}\,\bar{E}(z_1)\,z_1/\nu \simeq 20.$$

This means that the motion at z_1 is dominated by inertial terms, and becomes progressively more turbulent for $z > z_1$.

9. Discussion and conclusion

Schmidt & Milverton (1935) determined the critical Rayleigh number from the change in slope of the heat flux against Rayleigh number. This method has been employed in the present study; and the schlieren observations have indeed given evidence that the value of ϕ_0, corresponding to the change in slope of the current density, is the critical value for the onset of instability. In the motionless state, the current density varies like $\epsilon K\phi_0^2/d^3$, as long as the non-dimensional charge density on the injector remains constant, or is sufficiently high that the transport is limited by space charge ($\bar{Q}(0) > 5$). Since this is indeed the case, any change in the variation of the current density with ϕ_0 must be due to the onset of convection.

The experimental critical voltages give a value for the instability number $(T_c)_{\rm exp} = \epsilon\phi_c/\eta K$ which lies between 80 and 90, depending on the liquids used (see table 1), whereas $(T_c)_{\rm th} = 161$ (Atten & Moreau 1972). It was thought that this discrepancy might be attributed to an instability associated with finite perturbations. Indeed, a recent nonlinear stability analysis (Atten & Lacroix 1974) shows that, under subcritical conditions, a stable cellular motion may exist, with a fluid velocity equal to or greater than the velocity of the ions; and a critical value of 118 was obtained for $\bar{Q}(0) = 10$. Experimentally, the existence of two critical numbers, one associated with small disturbances, the other with finite-amplitude disturbances, has been demonstrated by the occurrence of a hysteresis loop in I against ϕ_0 near ϕ_c. The values of $(T_c)_{\rm exp}$ given in this paper correspond, however, to small perturbations, not to finite ones. At this stage of our work, we thus have no satisfactory explanation for the discrepancy between $(T_c)_{\rm exp}$ and $(T_c)_{\rm th}$.

As ϕ_0 is increased gradually beyond ϕ_c, the electric Nusselt number grows as $T^{\frac{1}{2}}$, then reaches its saturation value (figure 6). It has been verified experimentally that this transition from $Ne \propto T^{\frac{1}{2}}$ to $Ne \simeq$ const. is characterized by the number $(MR)_T \simeq 30$. This corresponds to a Reynolds number $Re \simeq w'(\frac{1}{2})\, d/\nu \simeq 10$, a value proposed by Moore & Weiss (1973) for the transition from viscous to nonlinear flow in the thermal convection problem. It was also shown that the extrapolation of the asymptotic state of high MR values to $(MR)_T$ yielded $\max w'(z) \simeq \frac{1}{3}M$. At a Reynolds number $\simeq 10$ the viscous and nonlinear terms are of the same order. But the viscous analysis will be rigorously valid only up to, say, a Reynolds number of order 1, which gives $(MR)_v \simeq 10$. From figure 6, we see that Ne begins to deviate from the law $T^{\frac{1}{2}}$ when MR reaches a value of about 12. It can also be deduced from this figure that viscous effects become negligible, and that the motion is probably fully turbulent when MR is about 180.

A condition for the validity of the law $Ne = (\frac{1}{3}M)^{\frac{1}{2}}$ is that $M \geqslant 3$. This critical value of M is also obtained from the velocity estimation ($w' \simeq \frac{1}{3}M$), which implies that, when $M < 3$, the fluid velocity is smaller than the ionic velocity. In this case, the velocity fluctuations may still produce charge fluctuations, but the effect on the charge transport will be small, and completely negligible when $M < 0{\cdot}1$. (A crude analysis then leads to $Ne \simeq 1 + \gamma M^2$.) Clearly, in this case the mean charge distribution will hardly be different from the distribution in the motionless state. A typical example of this is the corona effect observed in gases (already pointed out by Félici). In air, the ionic mobility is about $2\ {\rm cm^2\,(V\,s)^{-1}}$ and $(\epsilon/\rho)^{\frac{1}{2}} \simeq 2{\cdot}6\ 10^{-2}\ {\rm cm^2\,(V\,s)^{-1}}$. This gives a value of $M = 1{\cdot}3 \times 10^{-2} \ll 3$. The critical value $M = 3$ is an upper bound for all gases at moderate pressures; it is a lower bound for practically all liquids. Only in a few, very special cases can M take values lower than 3. One example is the injection of H^+ ions into water, for which $M \simeq 2{\cdot}5$.

Of course, the critical value $M = 3$ has a consequence for the state of motion immediately following instability. At the onset of instability, characterized by $T_c \simeq 90$, we have

$$(MR)_c = T_c/M;$$

	Thermal convection (high Pr numbers)		Electro-convection ($M > 3$)	
	Viscous or steady flow	Inertial or time-dependent flow	Viscous or steady flow	Inertial or time-dependent flow
Relative flux	$Nu \propto Ra^{\frac{1}{3}}$	$Nu \propto Ra^{0.278}$†	$Ne \simeq \left(\frac{T}{T_c}\right)^{\frac{1}{2}}$	$Ne \simeq (\frac{1}{3}M)^{\frac{1}{2}}$
Absolute flux	$Q \propto (\Delta T)^{\frac{4}{3}}$	$Q \propto (\Delta T)^{1.278}$	$I \propto \phi_0^{\frac{5}{2}}$	$I \propto \phi_0^2$
Velocity norm A	$A = \frac{w}{\kappa/d} \simeq Ra^{\frac{2}{3}}$	$A \simeq \frac{1}{3}Ra^{\frac{1}{2}}$‡	$A = \frac{w}{K\phi_0/d} \simeq \frac{T}{T_c}$	$A \simeq \frac{1}{3}M$
Relative flux as function of A	$Nu \propto A^{\frac{1}{2}}$	$Nu \propto A^{0.56}$	$Ne \simeq A^{\frac{1}{2}}$	$Ne \simeq A^{\frac{1}{2}}$

† From Chu & Goldstein (1973), $Pr = 7$; $10^5 \leqslant Ra \leqslant 10^8$.
‡ From Malkus (1954); Deardorff & Willis (1967).

TABLE 2. Comparison of the expressions for the relative flux and velocity for the thermal and electro-convection problems

and, if $M < 3$, we see that $(MR)_c > (MR)_T$. That implies that no stable convective motion can be observed. The motion is immediately nonlinear. That behaviour is already indicated in chlorobenzene, which has a value $M \simeq 5$, and in which no branch $Ne \propto T^{\frac{1}{2}}$ is distinguishable.

Finally, a more systematic comparison with the thermal problem reveals some interesting aspects. When we look just at the Nusselt number against stability parameter relations in both problems, we should be inclined to conclude that the basic phenomena in the two problems have little similarity. In the thermal problem, the Nusselt number grows steadily with increasing Rayleigh number, and exhibits successive transitions in the power of Ra. By contrast, in the electro-convection problem, we observe only one very marked transition, and afterwards the electric Nusselt number becomes independent of the stability parameter T. The latter saturation implies that the reference mobility current grows at the same rate as the convective current. This is because $q' \propto \bar{Q}$, and the velocity is proportional to the applied voltage. In the thermal problem, we have roughly $\theta' \propto \Delta T$, but w' has a constant reference velocity (for fixed d), so Nu grows with w' when ΔT and thus Ra is increased. Nevertheless, the absolute value of the current increases with applied voltage; and its dependence on the stability number T or applied voltage ϕ_0 is stronger than the dependence of the heat flux on Ra or ΔT. A more consistent picture is obtained when the variation of the Nusselt number with velocity norm A is examined. The relations

$$Nu \propto A^{\frac{1}{2}} \text{ and } Ne \propto A^{\frac{1}{2}}$$

seem to be valid in both problems, and in both states. These different variations are summarized in table 2. It should be noted that, as far as the velocity norm is concerned, the true relation is that kinetic energy is proportional to Ra. Only if the ratio of the vertically averaged root-mean-square values u' and w' is independent of Ra, may we take $A \propto Ra^{\frac{1}{2}}$. In the problem of time-dependent thermal

convection this is not strictly true. Also, the relation $Nu = f(Ra)$ in the inertial state of motion is a weak function of the Prandtl number. But this dependence is included in the coefficient of proportionality.

At very low Prandtl numbers, the situation is quite different. The dependence of the Nusselt number on Pr seems to be stronger. If Pr is low enough, no steady flow exists at $Ra > Ra_c$, and there is a direct transition from the state of no motion to a time-dependent and, depending on the value of Pr, to a fully turbulent flow. The Nusselt number in this case may approach 1, which means that the temperature distribution is no longer modified by the motion of the fluid. An equivalent situation is observed in the present problem when $M < 3$, as discussed above. From this it may be legitimate to conclude that the number M takes the role of the Prandtl number, not $1/R$, as might be deduced from a comparison of the governing equations.

REFERENCES

ATTEN, P. & GOSSE, J. P. 1969 Transient of one-carrier injections in polar liquids. *J. Chem. Phys.* **51**, 2804–2811.

ATTEN, P. & LACROIX, J. C. 1974 Stabilité hydrodynamique non linéaire d'un liquide isolant soumis à une injection unipolaire forte. *C. R. Acad. Sci.* B **278**, 385–387.

ATTEN, P. & MOREAU, R. 1972 Stabilité électrohydrodynamique des liquides isolants soumis à une injection unipolaire. *J. Mécan.* **11**, 471–520.

AVSEC, D. & LUNTZ, M. 1937 Tourbillons électroconvectifs dans une nappe *liquide*. *C. R. Acad. Sci.* **204**, 420–422.

BUDDE, W. 1962 *Appl. Opt.* **1**, 201–205.

CHU, T. Y. & GOLDSTEIN, R. J. 1973 Turbulent convection in a horizontal layer of water. *J. Fluid Mech.* **60**, 141–159.

DEARDORFF, J. W. & WILLIS, G. E. 1967 Investigation of turbulent thermal convection between horizontal plates. *J. Fluid Mech.* **28**, 675–704.

FÉLICI, N. 1969 Phénomènes hydro- et aérodynamiques dans la conduction des diélectriques fluides. *Rev. Gén. Electr.* **78**, 717–734.

FÉLICI, N. & SAUVIAT, M. 1972 Electrodialytic varnishes as ion injectors. *Proc. Int. Conf. Conduction and Breakdown in Dielectric Liquids*, Dublin, pp. 43–46.

HOPFINGER, E. J. & GOSSE, J. P. 1971 Charge transport by self-generated turbulence in insulating liquids submitted to unipolar injection. *Phys. Fluids*, **14**, 1671–1682.

HOPFINGER, E. J. & LACROIX, J. C. 1972 Hydrodynamic mechanisms of charge transport near the electrodes. *Proc. Int. Conf. Conduction and Breakdown in Dielectric Liquids*, Dublin, pp. 97–100.

KRAICHNAN, R. H. 1962 Turbulent thermal convection at arbitrary Prandtl number. *Phys. Fluids*, **5**, 1374–1389.

LACROIX, J. C. & TOBAZÉON, R. 1972 Experimental study of charge transfer phenomena in viscous fluids with single carrier injection. *Proc. Int. Conf. Conduction and Breakdown in Dielectric Liquids*, Dublin, pp. 93–96.

MALKUS, W. V. R. 1954 The heat transport and spectrum of thermal turbulence. *Proc. Roy. Soc.* A **225**, 196–212.

MOORE, D. R. & WEISS, N. O. 1973 Two-dimensional Rayleigh–Bénard convection. *J. Fluid Mech.* **58**, 289–312.

OSTROUMOV, G. A. 1954 *Zh. Tekh. Fiz.* **24**, 1915–1919.

SCHMIDT, R. J. & MILVERTON, S. W. 1935 On the instability of a fluid when heated from below. *Proc. Roy. Soc.* A **152**, 586–594.

SCHNEIDER, J. M. & WATSON, P. K. 1970 Electrohydrodynamic stability of space-charge-limited currents in dielectric liquids. I. Theoretical study. *Phys. Fluids*, **19**, 1948–1954.

SPIEGEL, E. 1962 On the Malkus theory of turbulence. *Mécanique de la Turbulence, Colloque International du CNRS*, no. 108.

STUETZER, O. M. 1962 Magnetohydrodynamics and electrohydrodynamics. *Phys. Fluids*, **5**, 534–544.

VERONIS, G. 1966 Large-amplitude Bénard convection. *J. Fluid Mech.* **26**, 49–68.

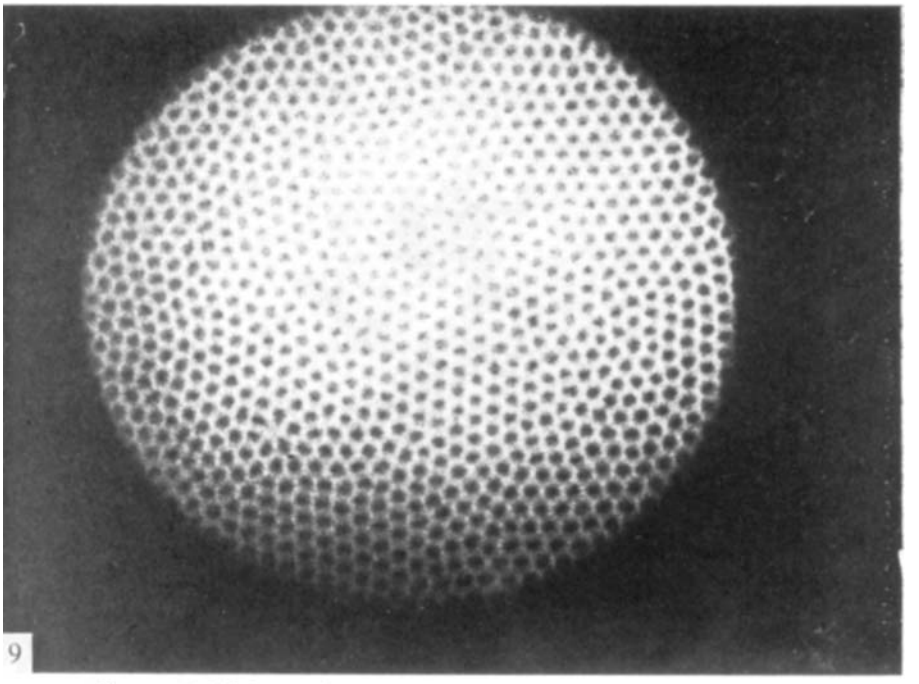

FIGURE 9. Schlieren photograph near critical conditions in pyralene 1460 ($d = 0{\cdot}3$ mm). $\phi_0 \simeq 1{\cdot}1\phi_c$, showing hexagonal structure.

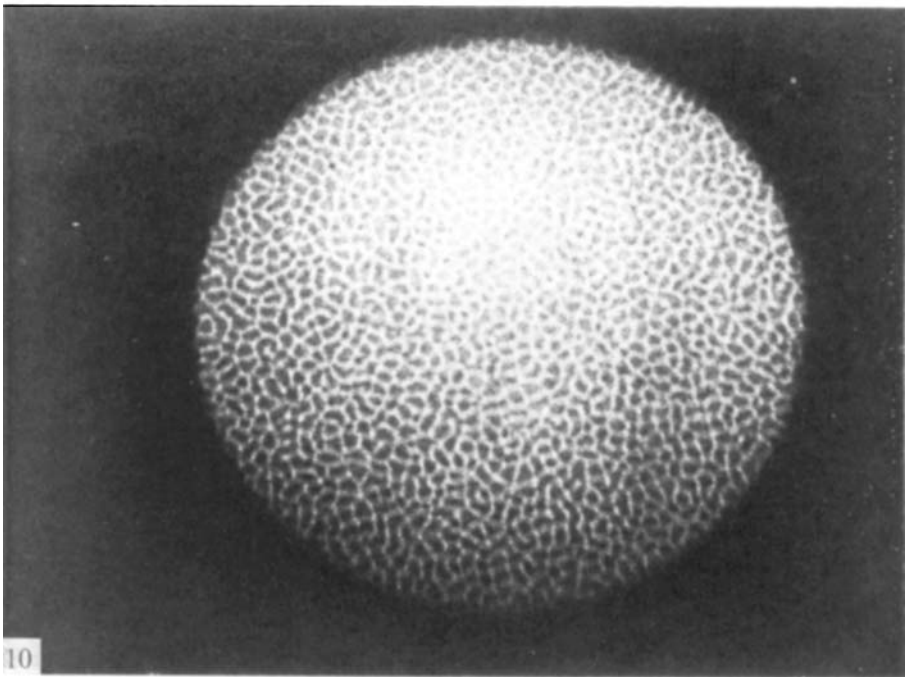

FIGURE 10. Schlieren photograph near critical conditions in pyralene 1460 ($d = 0{\cdot}3$ mm). $\phi_0 \simeq 2\phi_c$, corresponding to quasi-cellular motion.